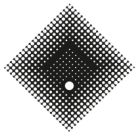
VICTORIA UNIVERSITY
MELBOURNE AUSTRALIA

AI-driven framework for accurate detection of Alzheimer's disease in EEG

This is the Published version of the following publication

Hemalatha, B, Venkatachalam, K, Siuly, Siuly and Cho, J (2026) AI-driven framework for accurate detection of Alzheimer's disease in EEG. Scientific Reports, 16 (1). p. 5509. ISSN 2045-2322 (In Press)

The publisher's official version can be found at
https://doi.org/10.1038/s41598-026-35184-3
Note that access to this version may require subscription.

Downloaded from VU Research Repository https://vuir.vu.edu.au/50099/

scientific reports

Check for updates

OPEN

AI-driven framework for accurate detection of Alzheimer's disease in EEG

B. Hemalatha[1]✉, K. Venkatachalam[2], Siuly Siuly[3] & Jaehyuk Cho[4]✉

Alzheimer's Disease (AD) is a rapidly growing neurodegenerative disorder that severely impairs cognitive function, particularly among older adults. Early detection is critical for timely intervention and effective management. While electroencephalography (EEG) provides a non-invasive, cost-effective tool with high temporal resolution for diagnosing Alzheimer's Disease (AD), traditional EEG-based approaches often struggle to extract informative features accurately from complex brain signals, thus limiting their diagnostic performance. This study addresses these challenges by proposing a novel artificial intelligence-based framework that integrates feature fusion with a Convolutional Long Short-Term Memory (Conv-LSTM) architecture. The model combines spectral features and deep learning-derived representations into a unified feature set, which is then processed by the LSTM network to capture both spatial and temporal patterns associated with AD. The proposed method achieves a classification accuracy of 99.8%, outperforming existing techniques and demonstrating its effectiveness in distinguishing between multiple stages of AD. Experimental results confirm the superiority of the fusion-based approach in learning high-level, discriminative features from EEG signals. This research represents a significant advancement in EEG-based Alzheimer's disease (AD) detection, with strong potential for enhancing early diagnostic systems. It supports the development of intelligent, scalable clinical tools for dementia screening and contributes to the broader effort to integrate AI into the diagnosis of neurodegenerative diseases.

Keywords Alzheimer's disease, Biomarker approaches, Deep learning, Early diagnosis, EEG data, Optimization

Alzheimer's disease (AD) is a degenerative neurological condition that gradually impairs memory, cognitive function, and the ability to perform everyday tasks. It is the most prevalent form of dementia, primarily affecting older individuals. This widespread disease profoundly impacts the quality of life of those affected, gradually diminishing their independence and their ability to carry out even basic activities. No treatment exists at this time for AD, and the median lifespan after diagnosis is 4.5 years. Mild cognitive impairment (MCI) is a preclinical stage of AD that exhibits only isolated cognitive abnormalities and may subsequently lead to AD[3–5]. This occurs because the symptoms of AD overlap with those of normal ageing or other illnesses, and a definitive diagnosis requires histological investigation of the brain or more complicated tests such as structural MRI[6].

Early detection and accurate diagnosis of AD are crucial for effective treatment and intervention strategies. Electroencephalography (EEG) is a non-invasive and cost-effective method for assessing brain activity, making it a promising tool for AD detection. However, interpreting EEG data and identifying true AD patterns from artifacts can be challenging. Also, its statistical properties change over time and make the model difficult to understand. This type problem needs adaptive algorithms to handle dynamic patterns. EEG data records multiple dimensionality data from multiple recordings and spatial complexity arises. This problem needs advanced feature extraction model due to the complexity and high-dimensional nature of the data. Therefore, there is a need for automated techniques that can effectively analyze EEG data and accurately detect Alzheimer's disease.

In recent years, EEG has gained popularity as a tool for identifying neurodegenerative diseases like AD[7–13]. The EEG is a non-invasive examination that provides recordings of electrical activity in the brain and can provide a proxy for the brain's physiological condition at multiple places on the patient's head. Those waves may

[1]Department of Information Technology, Dr. N.G.P. Institute of Technology, Coimbatore 641048, India. [2]Department of Computer Science and Engineering, Karunya Institute of Technology and Sciences, Karunya Nagar, Coimbatore 641114, India. [3]Institute for Sustainable Industries and Liveable Cities, Victoria University, Melbourne, Australia. [4]Department of Software Engineering and Division of Electronics and Information Engineering, Jeonbuk National University, Jeonju-si, Republic of Korea. ✉email: balanhemalatha83@gmail.com; chojh@jbnu.ac.kr

be broken down into frequency ranges corresponding to specific mental processes. Over the past few years, deep learning techniques have demonstrated remarkable achievements in diverse medical applications, ranging from computer-aided diagnosis to disease detection. Over the past few years, deep learning techniques have achieved outstanding results across a range of medical applications, from computer-aided diagnosis to disease detection.

The research problem addressed in this study is the automatic detection of Alzheimer's disease (AD) using EEG data by combining spectral and deep learning features. Spectral analysis of EEG signals involves extracting frequency-based features, such as power spectral density (PSD) and spectral entropy, to capture the characteristic patterns associated with AD. Meanwhile, deep learning offers powerful tools for automatically learning complex representations from raw data, enabling the discovery of hidden patterns in EEG signals. The novelty of this research lies in the fusion of spectral and deep learning features to leverage the complementary strengths of both approaches. By combining spectral features that capture specific frequency-related abnormalities in the brain with deep learning features that learn intricate representations, it is anticipated that the accuracy and robustness of Alzheimer's disease detection from EEG data will improve. Deep learning-based approaches for AD detection from EEG typically involve preprocessing raw EEG signals, extracting features, and classifying using deep neural networks. Preprocessing techniques may include filtering, artifact removal, and normalisation to enhance the standards and reliability of EEG data. Feature extraction methods aim to capture relevant temporal and spatial information from EEG signals, which can then be fed into simpler deep learning models for classification. By training deep learning algorithms on extensive EEG datasets from AD patients and normal controls, these models can learn to distinguish normal brain activity from abnormal patterns associated with AD. The developed models may be used to classify new EEG data and provide diagnostic information regarding the presence or progression of AD.

Applying deep learning techniques to EEG-based AD detection has significant potential to enhance diagnostic precision and effectiveness. It can help clinicians make more informed decisions, enabling early intervention and personalised treatment plans for patients. Additionally, deep learning models can help us understand the brain's functioning in AD and facilitate the development of novel therapeutic strategies. This paper explores the application of deep learning techniques to EEG-based dementia diagnosis. We investigate various architectures, preprocessing schemes, and feature extraction approaches to optimise model performance. This research assists doctors in early AD detection, creating a highly reliable and accurate deep learning-based solution, and contributes to ongoing research efforts in understanding and combating this devastating disease.

Research motivation

Most current EEG-based AD detection methods use predefined spectral or statistical features, which generally do not account for the complex spatiotemporal characteristics of brain activity. Deep learning models, however, have the potential to automatically find representations of the EEG that are indicative of AD, but they generally have higher computational requirements and lower interpretability than traditional models due to the need to process large amounts of raw EEG data. Many previous studies have employed either spectral or deep learning features alone, thereby failing to extract all of the possible useful information present in EEG signals.

The above mentioned reasons motivated this study to develop an adaptive, efficient and robust method for combining domain-specific spectral knowledge with deep learning derived features in order to provide interpretable and computationally feasible representations of EEG data while also improving the diagnostic accuracy, generalizability and practical utility of early Alzheimer's disease detection systems. This was achieved by fusing spectral and CNN-derived features and applying CLSTMs to model the temporal relationships between them.

Contribution of the research is as follows,

1. The hybrid feature fusion framework is proposed, integrating spectral-based EEG features and CNN features for capturing both frequency domain abnormalities and high-level spatial patterns related to Alzheimer's disease.
2. The CNN used for feature extraction has been optimized for extracting discriminative spatial features of the EEG signal without increasing the number of trainable parameters to avoid overfitting and reduce computation cost.
3. This proposed model employs a Convolutional Long Short-Term Memory (CLSTM) network to capture temporal dependencies in fused EEG features to learn spatio-temporal patterns essential for AD detection.
4. In comparison to conventional deep learning models that have large numbers of parameters to provide high classification performance, the proposed model uses only approximately 0.9 million trainable parameters, which makes it feasible to be implemented in real-world scenarios and deployed in real time.

Related works

Numerous research studies have been conducted to explore the early detection of Alzheimer's disease (AD) through the analysis of EEG signal data. Traditional methods for diagnosing AD early require manually extracting features from raw EEG recordings, followed by classification when necessary. These strategies may not align well with something as intricate as this. Due to its remarkable success in various identification tasks, deep learning has recently gained significant academic attention. The complex and nonlinear nature of EEG signals necessitates the creation of innovative methods for studying machine and signal processing. Recent advancements in deep learning methodologies have enhanced high-level abstraction techniques for automatically eliminating complex data characteristics. These deep learning approaches have been found to develop cutting-edge methods for widespread application in recent years, predominantly in image processing, natural language processing, voice processing, and video gaming. These techniques have also been applied in the biomedical sector.

Ieracitano et al.[25] employed a strategy to categorise EEG recordings in dementia, making them the most current authors to do so. To distinguish between AD, mild cognitive impairment (MCI), and healthy aging (HA), the authors utilise a novel combination of structures derived from Bispectrum analysis and a Continuous Wavelet Transform (CWT) time-frequency analysis. The findings indicate that this classification can achieve an accuracy of up to 89.22%. A review of EEG for AD detection was published by Cassani et al.[26], offering suggestions for further research in this field. The authors advocate creating large EEG datasets that are evenly distributed across demographic factors, including age, gender, participant count, and level of education. The study also calls for more precise and comprehensive explanations of how machine learning (DL) functions. For the three-class categorisation of AD, MCI, and HA, Ieracitano et al.[27] used 2D greyscale PSD images as input to a convolutional neural network, an example of a shallow machine learning technique. In contrast, the authors report that CNN achieved an accuracy of 83.33%.

There was a noticeable improvement in accuracy when utilising CNNs in this area. Nevertheless, the authors conclude that more than this approach is needed to diagnose AD. Magnetic Resonance Imaging (MRI), genetics, and clinical and biological materials are just some indicators that can be used to diagnose AD[14]. Biomarkers represent the raw data utilised in the diagnosis of AD. Selecting an appropriate biomarker is crucial given conflicting data on reliable options[15]. The diagnostic utility of computed tomography (CT) scans is enhanced by the capacity to distinguish spatial parameters, such as cortical thickness, brain volume, and brain surface area, following processing[16]. Tailored and deep learning abstraction approaches are applied to biomarkers to facilitate automated feature extraction. While neural networks such as CNNs and Transfer Learning Approaches are commonly used for Alzheimer's diagnosis[17], widely adopted automated pipelines can be applied as handcrafted approaches for processing biomarkers.

The pipeline employs a shallow CNN architecture to swiftly and accurately diagnose patients, classifying them globally (average, MCI, AD) and locally (VMD, MD, MoD)[18]. Additional methods for identifying AD include the Ensemble method and an ANN-based strategy. The ANN outperforms Gradient Boosting and the Voting Classifier[19] in long-term accuracy. The aim of a hybrid Deep Learning approach, incorporating the LSTM algorithm and MRI, is to distinguish cognitively healthy individuals from those with MCI for earlier diagnosis and treatment[20]. The most frequently used indicators are MRI and PET scans, and a wavelet-transform-based multimodality integration of both is implemented for early identification[21] in the Multimodality approach to AD diagnosis. The impact of fusing MRI with cross-sectional biomarkers is explored in early AD diagnosis using a hybrid deep-learning architecture composed of a 3D CNN and a bidirectional RNN[22].

Brain imaging in moderate MCI patients was used to investigate the many different kinds of ANNs that can potentially diagnose and foretell AD[23]. After careful evaluation of the topic, only the most pertinent articles were selected. Other approaches exist for classifying people with scalp EEG recordings into AD, MCI, and healthy control (HC) groups, including Alterations to convolutional neural networks (CNNs) and convolutional auto-encoder networks (Conv-AEs) for EEG deep learning (DL)[24]. These studies show there has been an undeniable advancement in EEG-based AD identification. In addition, recent developments in computer science have offered fresh information about the brain's collective behavior by seeking to clarify the principles driving the communication among neuronal and synaptic processes[28,29], which may assist in a more nuanced comprehension of the progression of neurodegeneration in AD.

Recent research has focused on closing the gap between computer models and their biological analogues in terms of efficiency and intelligence[29,30]. Therefore, models must consider the morphological aspects of neuronal motion and the overall scale of the human brain network to capture the brain's intricate structure. Several methods based on the simplified compartmental model have been introduced recently for this purpose, including Yang et al.[31]. Additionally, online learning and fault-tolerant operation are essential for the deployment of large-scale neuromorphic systems[32,33]. In the context of real-world methods for detecting AD, methodological choices hinder the widespread adoption of automated detection models. Clinical EEG acquisition techniques, visual examination and annotation of artefacts, and complex electrode montages are all integral to the process.

This article[35] addresses the application of deep learning in the medical field. A thorough review of various deep-learning algorithms for diagnosing Alzheimer's disease was conducted. Alzheimer's disease is described as a progressive brain disorder that gradually destroys memory. It is noted that the disease is common in older adults and is caused by dementia. In the article[36], deep learning approaches, such as convolutional neural networks (CNNs) and recurrent neural networks (RNNs), were used, with neuroimaging data processed without feature selection. These approaches yielded up to 96.0% accuracy for AD classification and 84.2% for MCI conversion prediction. This article[37] utilises pathways and target gene networks associated with confirmed miRNA biomarkers in AD diagnosis. Multiple models were created for diagnostics by leveraging the significant differences observed in miRNA expression between blood profiles. In this article[38], the detection of Alzheimer's disease was investigated using transfer learning in multi-class classification with brain medical resonance imaging (MRI). The objective was to classify the images into four stages: Mild Demented (MD), Moderate Demented (MOD), Non-demented (ND), and Very Mild Demented (VMD). Simulation results indicated that the proposed system model achieved an accuracy of 91.70%[39,40].

Based on the literature review, a research gap was identified in the automatic detection of Alzheimer's disease by fusing spectral and deep learning features from EEG data. While previous studies[41] have separately explored spectral analysis and deep learning techniques for Alzheimer's disease detection[27], there is a lack of research on effectively integrating these two approaches. The fusion of spectral features, which capture specific frequency-related abnormalities in EEG signals, with deep learning features, which learn complex representations, can potentially improve the accuracy and robustness of Alzheimer's disease detection[42].

The research work in[44] proposed hybrid models for AD detection. The model complexity is high due to the management of features in deep learning models. This research highlights the need for a separate feature handling model. Research[45] employs the synchrosqueezing transform for feature extraction and transfer learning

for classification. The model's accuracy and generalisability need improvement. Three different features[46]—statistical, time-domain, and frequency-domain—are tested with the SVM model. This result shows a significant gap in the need for feature fusion and processing when using a simpler deep learning model.

Significant advancement has occurred in research for the detection of Alzheimer's disease (AD) via EEG signals; however, there are still multiple issues that need resolution. Most existing algorithms use handcrafted spectral features or deep neural network architectures to capture the spatial aspects of the EEG signal. However, very little research has successfully combined the two types of analysis, and most algorithms exhibit high computational complexity, overfitting, and low generalizability across different EEG datasets. Although popular machine learning techniques such as support vector machines and random forests are commonly used, they often fail to capture the temporal characteristics of EEG signals that are essential for accurate AD detection. Also, currently, no comprehensive models exist that can provide the fusion of features (spatial and spectral) with a temporally based model in a computationally efficient format. The proposed FF-CLSTM model addresses these deficiencies and proposes a new method to improve the accuracy, robustness, and scalability of AD diagnosis from EEG data by combining spectral-based and CNN-extracted features with long short-term memory (LSTM) for spatio-temporal modeling.

Methods and materials

Problem formulation

The problem formulation of AD detection from EEG can be defined as a binary classification task, where the goal is to classify EEG signals as either belonging to individuals with AD or healthy individuals (non-AD). Mathematically, we can represent the problem as follows:

Given a dataset $D = \{(X_i, y_i)\}^{N_{\{i=1\}}}$, where X_i is the i-th EEG signal and y_i is its corresponding label indicating if Alzheimer's illness is present or not:

$X_i \in R^{T \times C}$ represents the EEG signal matrix, with T time samples and C channels/electrodes.

$y_i \in \{0, 1\}$ is the binary label, where $y_i = 1$ denotes AD and $y_i = 0$ denotes non-AD. The objective is to learn a classifier $f: R^{T \times C} \rightarrow \{0, 1\}$ that maps the input EEG signals to the corresponding AD or non-AD class labels. The classifier is specified by a set of parameters θ, learned from the training data. The problem can be formulated as an optimization task, aiming to find the optimal parameters θ^* that minimize a suitable loss function $L(\theta)$ over the training dataset:

$$\theta^* = argmin_\theta L(\theta) \tag{1}$$

The classification algorithm affects the selection of the loss function $L(\theta)$. Standard deviations of the projected likelihoods of classes and the actual labels are included. The trained classifier f can then be used to predict the Alzheimer's disease status of unseen EEG signals by evaluating $f(X)$ for new input data.

Proposed methodology

The research emphasizes the use of artificial intelligence (AI) techniques on EEG data for diagnosing AD. The innovation of our research is grounded in the comprehensive exploration of an automated method for diagnosing AD. This method employs a commercially available EEG recording device in conjunction with a novel deep learning-based categorization framework. We introduced a feature fusion approach that relies on spectral-based feature extraction and a strategically modified convolutional network. Additionally, we advanced the field by incorporating a Convolutional Long Short-Term Network (FF-CLSTM), effectively capturing spatial and temporal dependencies within the EEG data. This amalgamation of techniques represents a significant advancement in the AD diagnostic domain, enabling more accurate and reliable detection.

The study involves collecting EEG data from individuals, encompassing both healthy individuals and those diagnosed with Alzheimer's disease. Multiple electrodes are placed on the scalp to capture brain activity and ensure comprehensive data acquisition. Figure 1 shows the overall processing flow of the proposed model to diagnose Alzheimer's disease.

It is important to note that each electrode channel may have its own unique set of features, contributing to a comprehensive analysis. To enhance the effectiveness and productivity of the subsequent deep learning model, feature selection is performed. This step reduces the dimensions of the feature space and eliminates irrelevant or redundant features. Feature selection methods such as correlation analysis, mutual information, or statistical tests are commonly employed to identify the most informative features for AD detection.

From the pre-processed EEG data, spectral-based features are extracted. Power Spectral Density (PSD) is a commonly utilised spectral-based feature that quantifies power distribution across various signal frequencies. PSD provides insights into the strength or intensity of brain activity across different frequency bands. The pre-processed EEG data is input into a Convolutional Neural Network (CNN), a deep learning architecture renowned for extracting hierarchical and meaningful features from images. The CNN automatically learns discriminative features from the EEG data, capturing patterns and relevant representations for Alzheimer's disease detection. The features obtained from the spectral-based feature extraction and those extracted by the CNN are combined or fused. This fusion aims to leverage the complementary strengths of both approaches. The spectral-based features capture frequency-related abnormalities in the brain, while the CNN features capture more complex and higher-level representations. The classification algorithm learns from the fused features and makes predictions about whether the EEG data corresponds to Alzheimer's disease or not. The algorithm assigns a class label to the input data based on the patterns and features learned during training.

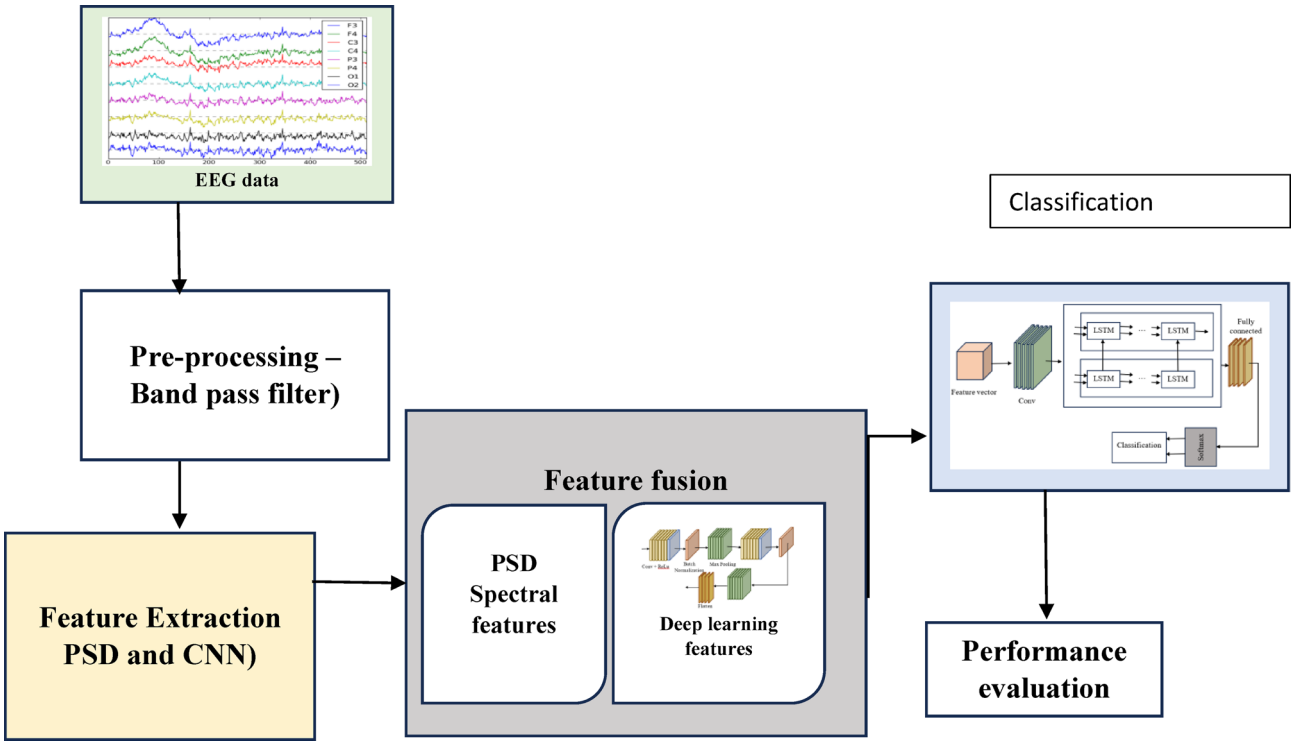

Fig. 1. The overall processing flow of the proposed model to diagnose Alzheimer's disease.

Category	Participants	Average MMSE	Mean age
Alzheimer's disease (AD)	36	17.75	66.4
healthy subjects (Cognitive Normal (CN))	29	30	67.9

Table 1. The average MMSE and the average age for the AD group.

Dataset acquisition

Resting-state, eyes-closed EEG recordings[1] from 88 participants are included in this data collection. There were 73 participants: 36 with AD, 23 with frontotemporal dementia (FTD), and 29 without any dementia (CN). The internationally renowned Mini-Mental State Examination (MMSE) served as the instrument for determining mental capacity and neuropsychological functioning. A lower MMSE score indicates more severe cognitive impairment, with scores ranging from 0 to 30. The median illness duration was 25 months, with the interquartile range (Q1–Q3) spanning from 24 to 28.5 months. No comorbidities associated with dementia have been observed among AD populations. FTD is not addressed in this research. Table 1 presents the average Mini-Mental State Examination scores for the Alzheimer's disease (AD) cohort.

Expert psychiatrists from the Second Department of Neurology at AHEPA General Hospital in Thessaloniki provided a recording. Nineteen 10–20 international system scalp electrodes and two mastoid baseline electrodes (A1 and A2) were used to record an EEG using a Nihon Kohden EEG 2100 medical device. Subjects sat quietly with their eyes closed throughout each recording, as instructed by the experimental procedure. Incorporating L2 regularization into the model's loss function imposes a penalty on large weights, incentivising the model to adopt smaller weights. This practice effectively mitigates the potential for extreme values contributing to overfitting. Enhancing the training dataset through the application of minor transformations, such as rotations, flips, and shifts, to the existing data expands the dataset's effective size. This augmentation strategy significantly improves model generalisation.

Data preprocessing

To enhance the quality of the signals, the raw EEG data undergoes preprocessing that includes noise removal, artifact elimination, and signal enhancement. Preprocessing steps typically involve filtering, resampling, and baseline correction techniques. The EEG data is pre-processed, after which the characteristics of interest are retrieved. Time-domain characteristics, frequency-domain information, and time-frequency characteristics are all taken into account.

To enhance the quality and practicality of EEG signals, reducing noise is crucial, as EEG recordings can be influenced by electrical noise, power-line hum, and environmental noise. The removal of such interference is accomplished through bandpass filtering, which confines the signal within a frequency range (typically between

0.5 and 50 Hz), eliminating frequencies outside this range. Furthermore, notch filters may also be utilised to remove power-line interference at 50–60 Hz, depending on the region.

Targeting physiological artifacts from eye blinks, muscle movements, and cardiac activity is vital for eliminating extremophys. Signals caused by these bodily changes are addressed using Independent Component Analysis (ICA) based approaches that isolate the artifacts without compromising the neural signals of interest. To enhance compatibility across datasets and reduce the computational burden, EEG signals are resampled to uniform rates. Downsampling high-frequency recordings to a consistent lower rate decreases file size without information loss, thereby improving processing speed.

Baseline correction is conducted to eliminate the slow drift or shifts in the signal baseline caused by the electrode and slow physiological processes. This involves calculating the mean of a reference period, which is subsequently subtracted from the entire signal to centre it around zero. Following preprocessing, smoothing, and normalisation techniques enhance the signal for further analysis, improving the signal-to-noise ratio. After completing these steps, appropriate features are identified across several domains. In the time domain, statistical features include mean amplitude, variance, and signal entropy. Frequency-domain features include spectral power and activity in specific bands, such as delta, theta, alpha, and beta, calculated using the Fourier Transform. EEG dynamics undergo various forms of analysis and classification, where time-frequency analysis methods like wavelet transforms highlight essential evolving signal characteristics, capturing the varying properties of signals.

Spectral-based feature extraction

Power Spectral Density (PSD) is a commonly used spectral-based feature that quantifies the distribution of power across different frequencies in a signal. In this study, we employed PSD techniques to extract key features from EEG signals, as PSD effectively reveals the frequency composition and relative power distribution across different EEG bands. The power spectral density at a specific frequency f is calculated using the Fourier Transform of the EEG signal. The squared magnitude of the Fourier Transform represents the power at each frequency component. Mathematically, the PSD is calculated as,

$$PSD\,(f) = |X\,(f)|^2 \tag{2}$$

where PSD(f) represents the power spectral density at frequency f, and $X\,(f)$ is the Fourier transform of the EEG signal at frequency f. To estimate the PSD, various techniques can be used, such as the Fast Fourier Transform (FFT), which efficiently calculates the Discrete Fourier Transform (DFT). The EEG signal is divided into multiple overlapping segments, and each segment is transformed using the FFT algorithm.

Spectral-based features (such as Power Spectral Density (PSD), spectral entropy, and band power) are calculated from the EEG signals prior to processing the EEG signals through the CNN architecture. The spectral-based features contain frequency domain information which help identify frequency specific abnormalities in AD. These spectral-based features are then combined with the CNN-derived features to produce a unified feature vector for classification.

The power spectra of individual segments are then averaged to gain an evaluation of the PSD. The PSD provides insights into the power distribution across different frequency bands. It helps identify frequency components associated with specific brain activities or abnormalities. For example, the PSD can reveal increased power in specific frequency bands, such as theta or delta, in individuals with neurological disorders like Alzheimer's or epilepsy. The feature extraction methods are shown in Fig. 2.

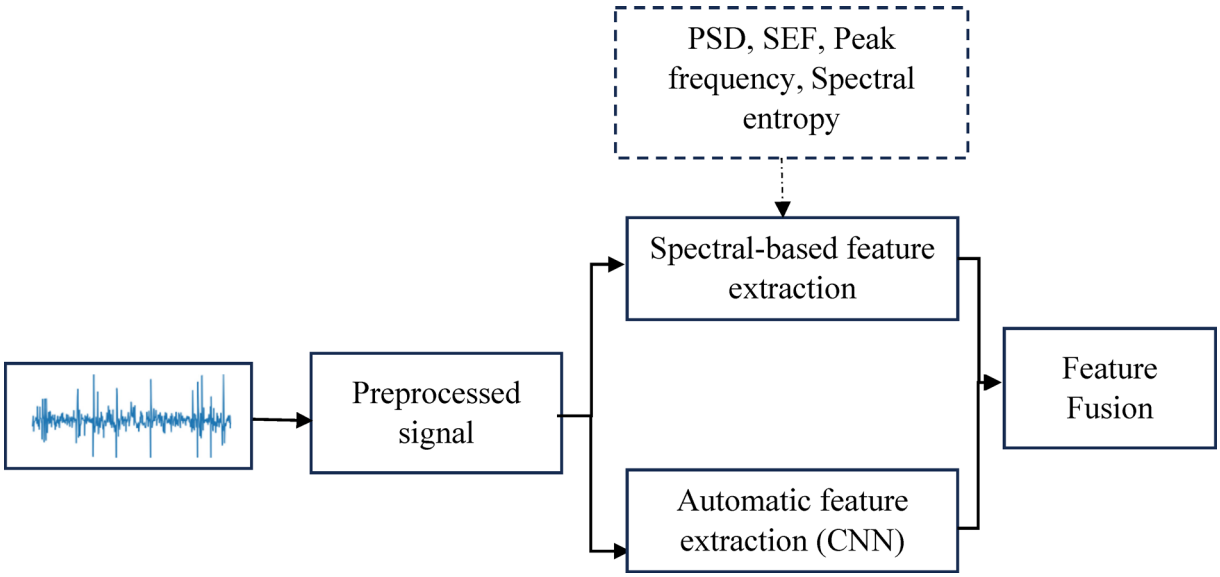

Fig. 2. Feature Extraction techniques.

Analyzing the PSD of EEG signals can involve examining specific frequency ranges, comparing power ratios between different frequency bands, or investigating changes in the power spectrum over time. Band power represents the power of EEG signals within specific frequency bands. It can be calculated by integrating or summing the power spectral density (PSD) values within a particular range of frequency. For example, the delta band power (0.5–4 Hz) can be calculated as,

$$Delta\ Band\ Power = \int_{flow}^{fhigh} PSD_n\left(f\right) \tag{3}$$

The speed at which a specific percentage of the overall strength of an EEG signal resides is known as the Spectral Edge Frequency (SEF). It can provide information about the dominant frequency range in the signal. The SEF can be calculated using a cumulative power distribution and a predefined threshold, such as 95% of the total power:

$$SEF = frequency \qquad where\ Cumulative\ power \geq Threshold \tag{4}$$

Peak frequency corresponds to the frequency at which the highest power or amplitude is observed in the EEG signal. It can be determined by identifying the frequency bin or bin range with the maximum power spectral density value. Spectral entropy measures the complexity or randomness of the frequency content in the EEG signal. It can be calculated using the power spectral density values and the Shannon entropy formula,

$$Spectral\ entropy = -\sum_{i=1}^{N} P(f_i)log_2(P\left(f_i\right)) \tag{5}$$

where N is the number of occurrence bins, $P\left(f_i\right)$ is the normalized power at the i-th bin associated with a certain the rate, and then summing up over all sectors. These spectral-based features provide insights into the frequency characteristics of EEG signals and are useful for various applications, including brain-state analysis, sleep staging, and disease detection. The choice of specific features may depend on the research objectives and the frequency bands of interest. The root-squared second- and fourth-order moments are statistical measures used to characterize the shape or distribution of a signal. In the context of EEG analysis, these moments helps us understand the temporal characteristics of the EEG signal. Hjorth[34] claims that the second time period can be used as power; however, this is followed by a frequency-domain shift denoted by $h^2P\left[h\right]$.

$$\bar{n}_1 = \sqrt{\sum_{i=0}^{M-1} h^2P\left[h\right]} = \sqrt{\frac{1}{M}\sum_{i=0}^{M-1}\left(kX\left[h\right]\right)^2} = \sqrt{\sum_{k=0}^{M-1}\left(\Delta\, x\left[k\right]\right)^2} \tag{6}$$

When this process is repeated, we get the time:

$$\bar{n}_4 = \sqrt{\sum_{i=0}^{M-1} h^4P\left[h\right]} = \sqrt{\sum_{k=0}^{M-1}\left(\Delta^{\,2}x\left[k\right]\right)^2} \tag{7}$$

To reduce the noise impact on all moment-based features, a power modifier is used to standardize the field of n_0, n_2, and n_4 in the following way:

$$n_0 = \frac{\bar{n_0}^{\lambda}}{\lambda}\ ,\ n_2 = \frac{\bar{n_2}^{\lambda}}{\lambda}\ ,\quad n_4 = \frac{\bar{n_4}^{\lambda}}{\lambda} \tag{8}$$

The value used in experiments is $\lambda\ = 0.1$. Thus, the first three characteristics retrieved from these variables are as given.

$$f_1 = log\left(n_0\right), \tag{9}$$

$$f_2 = log\left(n_0 - n_2\right), \tag{10}$$

$$f_4 = log\left(n_0 - n_4\right), \tag{11}$$

Deep learning based feature extraction

Feature extraction using Convolutional Neural Networks (CNNs) involves leveraging the network's capability to acquire knowledge independently from information and identify useful characteristics. CNNs are particularly effective for processing spatially structured data as shown in the Fig. 3, This makes them useful for examination of visual data, including EEG analysis where the spatial arrangement of electrode channels is important. EEG data is typically represented as a multi-channel time-series, where each channel corresponds to a specific electrode location. To feed EEG data into a CNN, it must be reshaped into a suitable input format. For instance, the input can be structured as a 2D matrix with channels representing the input depth, and the time-series samples forming the width and height dimensions.

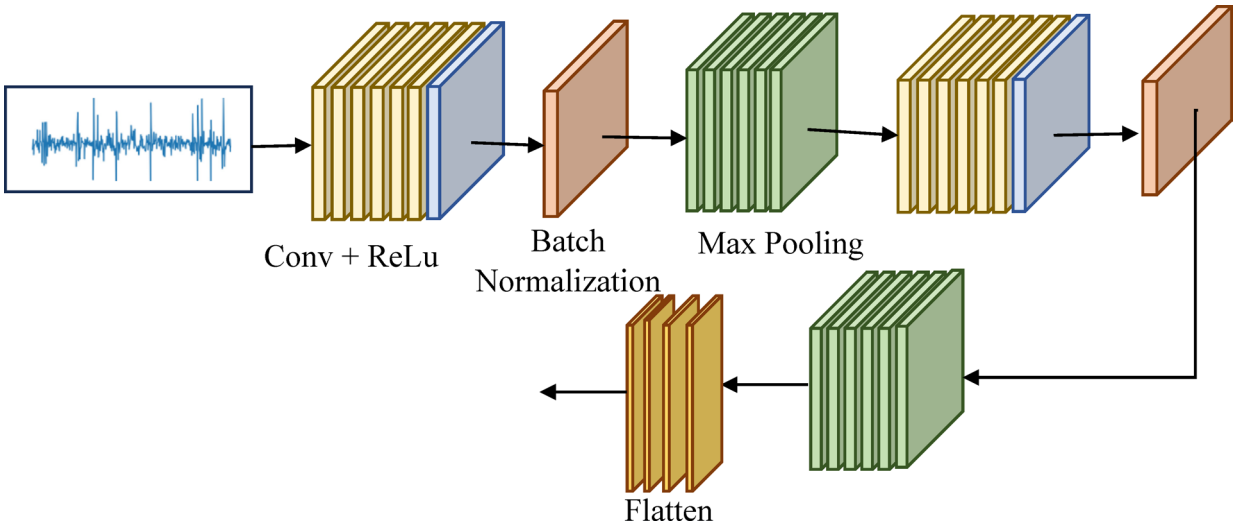

Fig. 3. Automatic Feature extraction module.

CNNs rely on their convolutional layers[47,48] above anything else that perform feature extraction. These different layers process the provided data through a series of tuneable filters (kernels), convolving them across the input volume to produce feature maps. Each filter captures specific local patterns or features. Convolutional layers are responsible for detecting various spatial patterns in the EEG data, such as temporal relationships or frequency-specific information. A visualization of features results from this process or a convolutional feature.

$$conv(I,F)_{i,j} = \sum_{l=1}^{L}\sum_{m=1}^{M} I_{i+l-1,j+m-1} \cdot F_{l,m} \tag{12}$$

where I represents the input data, F represents the filter, and the subscripts i, j, m, and l denote the spatial indices of both the input and the filter. Convolutional Layers (Conv2D): Filters (kernels) are applied to detect spatial features within the EEG input data. Max Pooling Layers used to reduce the dimensionality of the feature map produced in the previous layer while retaining the most important spatial features.

Activation functions introduce non-linearities to the CNN, enabling it to model intricate connections within the data. ReLU and its variations, Leaky ReLU and Parametric ReLU, are popular CNN activation functions due to their ability to convert negative numbers to zero. Activation functions facilitate a better understanding of non-linear representations and enhance the model's capacity to capture complex features.

$$A_{i,j} = f\left(conv(I,F)_{i,j}\right) \tag{13}$$

where A represents the output of the activation function and f denotes the activation function. Pooling layers are typically inserted after convolutional layers to down-sample and decrease the spatial dimensions of the feature maps while preserving the most salient features. Max pooling is a popular technique that selects the maximum value within each pooling region, effectively reducing the feature map size. Pooling layers help increase the model's robustness to small spatial variations and reduce the number of parameters in subsequent layers. After the CNN layers, the feature maps must be transformed into a suitable representation for fusion with the spectral-based features. This can be achieved by flattening the feature maps into a vector or applying pooling operations to reduce their dimensions while preserving the essential information. Following the convolutional and pooling layers, fully connected layers are added to capture high-level representations by integrating the spatially extracted features. As shown in Table 2, these layers are similar to those in traditional neural networks, connecting all neurons from the preceding layer to the current layer. The fully connected layers learn complex combinations of features and map them to the target output classes.

Activation functions such as softmax are essential for enabling fully connected layers to generate the final class probabilities or regression values. The choice of activation function relies on the specific task and the intended output format. By stacking and interleaving these layers, CNNs can effectively learn hierarchical representations of the input EEG data, automatically extracting discriminative features relevant to the given mission.

Feature fusion

Feature fusion refers to the combination of various sets of features to create a unified feature representation. When combining spectral-based features with features extracted by a CNN, several fusion strategies can be employed to capture both spectral information and high-level spatial patterns.

Spectral-Based Feature Extraction is employed to derive spectral-based features from EEG signals using techniques such as power spectral density (PSD), spectral entropy, or band power calculations. These features

Layer (type)	Output shape
conv2d_1 (Conv2D)	(None, 224, 224, 16)
conv2d_2 (Conv2D)	(None, 224, 224, 32)
max_pooling2d_1	(None, 112, 112, 32)
conv2d_3 (Conv2D)	(None, 112, 112, 32)
conv2d_4 (Conv2D)	(None, 112, 112, 64)
max_pooling2d_2	(None, 56, 56, 64)
conv2d_5 (Conv2D)	(None, 56, 56, 64)
conv2d_6 (Conv2D)	(None, 56, 56, 128)
max_pooling2d_3	(None, 28, 28, 128)
conv2d_7 (Conv2D)	(None, 28, 28, 128)
conv2d_7 (Conv2D)	(None, 28, 28, 128)
max_pooling2d_4	(None, 14, 14, 128)

Table 2. CNN model layer wise configuration details.

capture the frequency content and the distribution of power across different frequency bands. CNN-Based Feature Extraction[49] involves applying a CNN architecture to the pre-processed EEG data, enabling the network to learn spatial patterns and extract high-level features automatically. The CNN may consist of convolutional layers, activation functions, pooling operations, and potentially other components, such as fully connected layers.

Input:

- Spectral-based features: $F_{feature}$ (size: $N\ x\ M$)
- CNN extracted features: F_{cnn} (size: $N\ x\ K$)

Output:

- Fused features: F_{fused} (size: $N\ x\ (M\ +\ K)$)

Algorithm:

1. **Initialize** an empty matrix for the fused features:

$$F_{fused} = []$$

2. **For** each row i **in** $F_{spectral}$ and F_{cnn}:

a. Concatenate the spectral-based features $F_{spectral}\ [i]$ and CNN features $F_{cnn}\,[i]$ element-wise:

$$Fused_{row} = concatenate(F_{spectral}\ [i], F_{cnn}\,[i])$$

b. Append the $Fused_{row}$ to the F_{fused} matrix:

$$F_{fused} \cdot append(Fused_{row})$$

End for

3. **Return** the fused features F_{fused}.

Algorithm 1. Feature fusion of spectral-based feature extraction and features extracted by CNN

Element-wise feature fusion combines features extracted from different methods or sources by applying element-wise operations on corresponding feature vectors. In the case of combining spectral-based features and features extracted by a CNN, the fusion can be performed element-wise. The two feature vectors:

Spectral-based feature vector:

$$F_{spectral} = [f_1,\ f_2,\ f_3,\ \ldots,\ f_n] \tag{14}$$

From EEG, CNN takes 20 feature, then $F_{spectral} \in \mathbb{R}^{NX20}$.

CNN-extracted feature vector:

$$F_{CNN} = [c_1, c_2, c_3, ..., c_n] \tag{15}$$

Where dimensions are $F_{cnn} \in \mathbb{R}^{NX25088}$.

Element-wise addition for fusion can be represented as:

$$Fused_{row} = concatenate\,(F_{spectral}[i], F_{cnn}[i]) \tag{16}$$

Where fused dimension $F_{cnn} \in \mathbb{R}^{NX25108}$.

In this equation, the corresponding elements of the spectral-based feature vector and the CNN-extracted feature vector are combined to create the fused feature vector. This fusion process enhances representation power by merging the frequency information captured by the spectral-based features with the spatial patterns learned by the CNN[47,48]. It is important to note that the dimensionality of the feature vectors must match; that is, they should have the same number of elements to enable element-wise fusion. If the dimensions differ, appropriate preprocessing steps, such as dimensionality reduction or feature selection, can be applied to align the feature vectors before fusion. After the fusion, the resulting feature vector can serve as input for further processing, such as classification or regression tasks, leveraging the combined information from both spectral-based and CNN-extracted features, which could potentially lead to improved performance and a richer feature representation.

Classification

Convolutional Long Short-Term Memory (CLSTM) is an artificial intelligence design that combines the strengths of convolutional layers for spatial processing with LSTM layers[47] for temporal modelling. It is commonly utilised for sequence data analysis, including time-series and spatiotemporal data. When applied to classification tasks using fused features, CLSTM leverages the combined information to capture spatial and temporal dependencies in the data. The fused feature vector, obtained through element-wise feature fusion as described earlier, serves as the input to the CLSTM network. This fused feature vector contains the integrated information from the spectral-based features and the features extracted by the CNN.

The initial part of the CLSTM network consists of one or more convolutional layers. These layers are responsible for capturing spatial patterns and local dependencies within the fused feature vector. The input is filtered using a series of evolvable filters in the convolutional layers, extracting relevant features through sliding windows and convolution operations. Following the convolutional layers, one or more LSTM layers are employed. LSTM layers are specifically designed to model temporal dependencies in the data. They incorporate memory cells that retain information over varying time steps, allowing the network to learn long-term dependencies. The LSTM layers process the sequential nature of the fused feature vector, capturing temporal patterns and relationships. After the LSTM layers, one or more fully connected layers can be added to the network. These layers further transform the learned features and enable the network to make class predictions. The fully connected layers can also introduce non-linearities through activation functions to enhance the network's discriminative power.

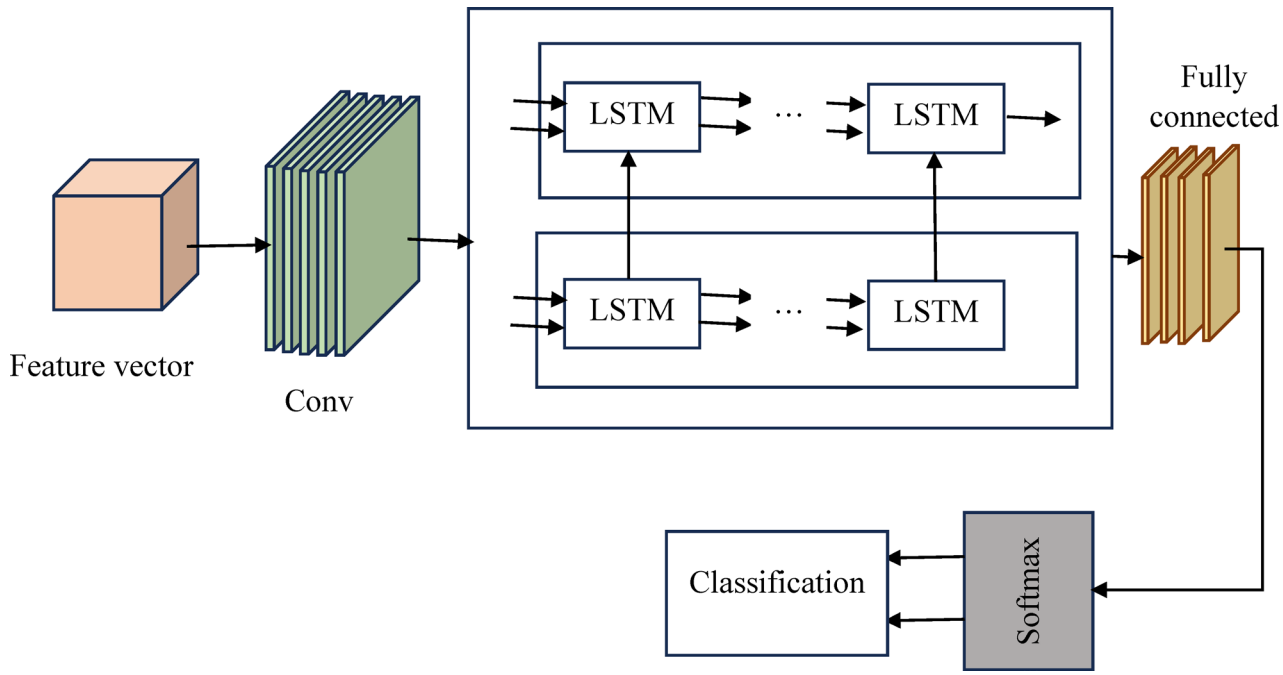

Fig. 4. CLSTM architecture for Alzheimer's disease detection.

For classification tasks, a CLSTM network's output layer commonly employs a softmax activation function as shown in the Fig. 4. It generates a distribution of chance over the classes, with weights assigned to each class based on how likely it is that the input sequence falls into that class. During training, the parameters of the CLSTM network are optimized using backpropagation and gradient-based optimization algorithms, such as Adam, to minimize a loss function, such as cross-entropy loss. By combining the strengths of convolutional layers and LSTM layers, CLSTM models can effectively capture spatial and temporal patterns in fused feature representations. This allows for improved classification performance, especially when dealing with spatio-temporal or sequential data. Through ongoing learning, LSTM units take on the temporal features of data at varying time steps T. There are primarily three types of gates involved in the process: an input gate, a memory gate, and an output gate. Data storage and transmission in the network of long- and short-term memory are regulated by the following three gates:

The fgt_{gt}forgetting gate is built with a Sigmoid neural network layer followed by a per-bit multiplication. The k_{t-1} indicates the state of the preceding hidden layer. Data is being entered using I_t. The b_{ft} value acts as an offset. The symbol for the Sigmoid function is.

$$fgt_{gt} = \sigma\left(w_{fgt} \cdot \left[k_{t-1},\ I_t\right] + b_{fgt}\right. \tag{17}$$

In contrast to the forgetting gate, the memory gate determines which of the newly input and −1 values to retain. Out-of-selective memory is represented by Mgt_t.

$$igp_{gt} = \sigma\ \left(w_{igp} \cdot \left[k_{t-1},\ I_t\right] + b_{igp}\right) \tag{18}$$

$$Mgt_{gt} = I_t * tanh\left(w_{mgt} \cdot \left[k_{t-1},\ I_t\right] + b_{mgt}\right) \tag{19}$$

In this step, we'll settle on the results that will be considered the state's output. Then, we feed in the signal I_t at time t. Following this, the relevant output signals are derived using the Equations.

$$opg_{gt} = \sigma\ \left(w_{opg} \cdot \left[k_{t-1},\ I_t\right] + b_{opg}\right) \tag{20}$$

$$k_t = opg_{gt} * tanh\left(Mgt_{gt}\right) \tag{21}$$

When the feature map traverses multiple LSTM time steps, the goal is to learn the anomalous region with less data and greater nuance by concurrently connecting the cell outputs of distinct time steps. The second LSTM layer takes its input from the output of the first layer. This may also spatially associate data from each time period across an extended range in a manner similar to connecting the entire dataset with reliable temporal associations. When the CNN is used as input to an LSTM, it acts as a range restrictor, reducing the retrieval window. Simultaneously, the LSTM retains the capability to perform internal temporal data prediction within each small time segment. To further expedite training and reduce sensitivity between convolutional layers and irregularities, a batch normalization layer is deployed, as indicated in Table 3, to standardise input results. Additionally, to enhance the generation of abnormal signal, a dropout layer is incorporated into the fully connected layers. In the final segment of the hidden layer, which is responsible for distinguishing signals, fully connected layers are employed. Ultimately, the deep learning layer that determines the categorisation choice is fully connected.

Temporal relationships are modeled using convolutional long short-term memory (CLSTM) models to identify the temporal dependencies after the features are combined. CNN's spatial processing and LSTM's temporal processing are used in a CLSTM to produce a model that can identify both spatial and temporal processes in the EEG signal. he first layers of the CLSTM model are Conv1D layers that process the fused feature sequences, where they learn to detect local spatial dependencies between different points in time. The LSTM

Layer (type)	Output shape
conv1d_1	(None, 100, 256)
max_pooling1d_1	(None, 50, 256)
dropout_1	(None, 50, 256)
conv1d_1	(None, 50, 128)
max_pooling1d_4	(None, 25, 128)
dropout_2	(None, 25, 128)
lstm_1	(None, 25, 64)
lstm_2	(None, 32)
dense_1	(None, 250)
dense_2	(None, 250)
dropout_3	(None, 250)
dense_3	(None, 3)

Table 3. CLSTM layer-wise configuration.

layers then identify longer term temporal dependencies, by maintaining memory state across several time steps as sequential data is processed and are essential to identifying how EEG patterns evolve over time.

Results and discussion

We have implemented the algorithm in Python and checked its performance. The available dataset is divided into three subsets: training set, testing set, and validation set. The training set comprises 60% of the data, which will be used to train the model. The testing set consists of 20% of the data and will evaluate the model's performance on unseen data. The remaining 20% of the data is allocated to the validation set, which will be used for fine-tuning the model and selecting hyperparameters. We have evaluated performance using ROC_AUC_Score, f1_score, and accuracy. Accuracy is defined as the percentage of correctly identified applications.

A classification model's efficacy may be measured in terms of its precision. It is the proportion of positive instances (true positives) to the total number of positive cases predicted by the model (true positives plus false positives). Recall measures the percentage of requested results that were returned.

To characterize the model, more than its precision is needed. The ROC_AUC estimates the area under the receiver operating characteristic curve for inter-class discrimination ability. The higher the ROC_AUC, the better the performance. An F-measure provides a graphical representation of the compromise between recall and accuracy. Training parameters are included in Table 4.

Trainable parameters

The trainable parameters in this proposed model is 0.9 million parameters contributed by the convolutional layers, LSTM layers, and fully connected layers. The convolutional layers contribute parameters in proportion to the number of filters, the kernel sizes used, and the number of input channels. The LSTM layers introduce trainable parameters for the gate weights and memory cells. Finally, the fully connected layers contain parameters which transform the learned representation into output classes.

This hybrid CNN-CLSTM architecture uses 0.9 million trainable parameters. The relatively modest parameter count of the model, despite its CNN-CLSTM architecture, is largely due to the application of pooling layers, feature fusion, and dimensionality reduction before temporal modelling. These mechanisms help prevent the model from overfitting the small EEG datasets used for training and enable fast training.

Computational overhead

In terms of the computational complexity of the model, the primary layers are the convolutional and LSTM operations. The convolutional layers perform $O(H \times W \times K \times C)$ operations per layer where H and W denote the spatial dimensions of the input data, K denotes the size of the kernels, and C denotes the number of filters. The LSTM layers contribute $O\left(T \times D^2\right)$ complexity where T represents the sequence length, and D denotes the hidden state dimension.

Max-pooling layers are used throughout the model to progressively down-sample the feature maps produced by each convolutional layer. Batch-normalization is also used throughout the model to accelerate convergence during training. Dropout layers are used throughout the model to both improve efficiency and to prevent co-adaptation between neurons during training.

Training and evaluation of the model were performed using a standard GPU-enabled computing environment. Training converged quickly to an acceptable solution. The modular nature of the CNN-fusion-CLSTM architecture allows for the scalability of the model by changing the number of filters, LSTM units, or the sequence length depending upon the amount of available computation resources. As such, the proposed method may be scaled up to accommodate larger datasets that are deployed in resource-constrained computing environments.

Performance analysis

The Statistical evaluation of performance is provided in Table 4. Our proposed model achieves higher accuracy and a superior F1 score compared to the supervised deep learning method. Table 5 displays the performance results of AD detection across various models. It details the outcomes of different models concerning precision,

Hyperparameter	Value
Optimizer	Adam
Learning rate	0.001
Batch size	32
Number of epochs	200
Loss function	Categorical cross-entropy
Activation functions	ReLU, Softmax
Dropout rate	0.5
Weight initialization	He normal
Early stopping	Patience = 3
Normalization	Batch normalization

Table 4. Training parameters of the model.

Models	Class	Accuracy	Sensitivity	Specificity	Precision	F1 score	ROC area value
FF- CLSTM	0		1.00	0.99	0.99	0.99	1.00
	1		0.99	0.99	1.00	0.99	0.99
	Overall	99.8%					
CLSTM	0		0.96	0.96	0.97	0.96	0.95
	1		0.98	0.96	0.98	0.97	0.94
	Overall	97%					
Conv2D + LSTM	0		0.93	0.93	0.94	0.92	0.90
	1		0.96	0.96	0.97	0.97	0.92
	Overall	95%					
CNN	0		0.94	0.95	0.95	0.95	0.95
	1		0.95	0.95	0.96	0.95	0.94
	Overall	95%					
LSTM	0		0.92	0.91	0.92	0.93	0.92
	1		0.94	0.90	0.93	0.92	0.91
	Overall	92%					

Table 5. Performance result of AD detection through the proposed models.

Model	Accuracy (%)	Precision (%)	Recall (%)	F1-score (%)	AUC (%)
FF-CLSTM	95.3 ± 2.1	94.5 ± 2.3	95.8 ± 1.8	95.1 ± 1.9	0.97 ± 0.02
SVM	90.1 ± 2.4	88.7 ± 3.0	89.5 ± 2.6	89.1 ± 2.7	0.93 ± 0.03
CNN-only	92.6 ± 2.0	91.4 ± 2.2	93.2 ± 2.0	92.3 ± 2.1	0.95 ± 0.02
LSTM-only	91.3 ± 2.2	90.2 ± 2.5	92.4 ± 2.1	91.3 ± 2.3	0.94 ± 0.02

Table 6. Statistical evaluation of performance.

recall, F1 score, and accuracy for classification. The models assessed in the table include FF-CLSTM, CLSTM, CNN, and LSTM. With scores of 0.99 and 1.00 for class 0, the FF-CLSTM model successfully recognised instances of class 0. It could accurately identify instances belonging to class 1 with a precision of 1.00 and a recall of 0.99. The F1 score, which incorporates both precision and recall, was 0.99 overall. The FF-CLSTM model achieved an overall accuracy of 99.8%.

The CLSTM model accurately identified class 0 instances with 0.97 accuracy and 0.96 recall. It could accurately identify cases belonging to class 1 with a precision of 0.98 and a recall of 0.98. F1-scores for class 0 were 0.96, and F1-scores for class 1 were 0.97. The CLSTM model achieved an overall accuracy of 97%. The CNN model accurately categorized examples into classes 0 and 1, achieving precisions of 0.95 and 0.96, respectively. Class 0 had a recall of 0.94 and class 1 had a recall of 0.95. Both class 0 and class 1 F1 scores were 0.95. The CNN model achieved an overall accuracy rate of 95%. Class 0 examples were identified with a precision of 0.92 using the LSTM model, and class 1 instances were identified with a precision of 0.93 using the model. Recall percentages for class 0 were 0.92, and class 1 was 0.94. Class 0 had an F1-score of 0.93, whereas class 1 had an F1-score of 0.92. The LSTM model achieved an overall accuracy rate of 92%. Table 6 presents a statistical evaluation of the models' performance.

In Fig. 5, the accuracy of various models for Alzheimer's disease (AD) detection is presented. The results demonstrate the effectiveness of utilizing feature fusion in combination with the CLSTM (Convolutional Long Short-Term Memory) architecture. CLSTM with feature fusion achieved an impressive accuracy of 99.8%, as shown in Fig. 5a. This indicates that the combination of spatial processing from convolutional layers and temporal modeling from LSTM layers, along with the integration of fused features, significantly contributed to the model's ability to classify Alzheimer's disease cases accurately. The feature fusion process likely enhanced the model's representation power by combining information from multiple sources.

From Fig. 5b In contrast, CLSTM without feature fusion achieved a slightly lower accuracy of 97%. This suggests that the absence of feature fusion reduced performance compared to the CLSTM model with feature fusion. The fused features likely provided additional discriminative information that aided in distinguishing between Alzheimer's disease and healthy cases. The CNN model, as shown in Fig. 5c, which solely relies on convolutional layers for feature extraction, achieved an accuracy of 95%. Although CNNs are powerful in capturing spatial patterns, the absence of LSTM layers for modelling temporal dependencies might have limited their ability to fully exploit the sequential nature of the data. The LSTM model, which focuses solely on temporal modelling, achieved an accuracy of 92%, as shown in Fig. 5. While LSTM layers are effective in capturing long-term dependencies, the absence of convolutional layers may have limited the model's ability to capture spatial patterns present in the data.

In Fig. 6, the loss values for different models are presented to evaluate their performance in Alzheimer's disease detection.

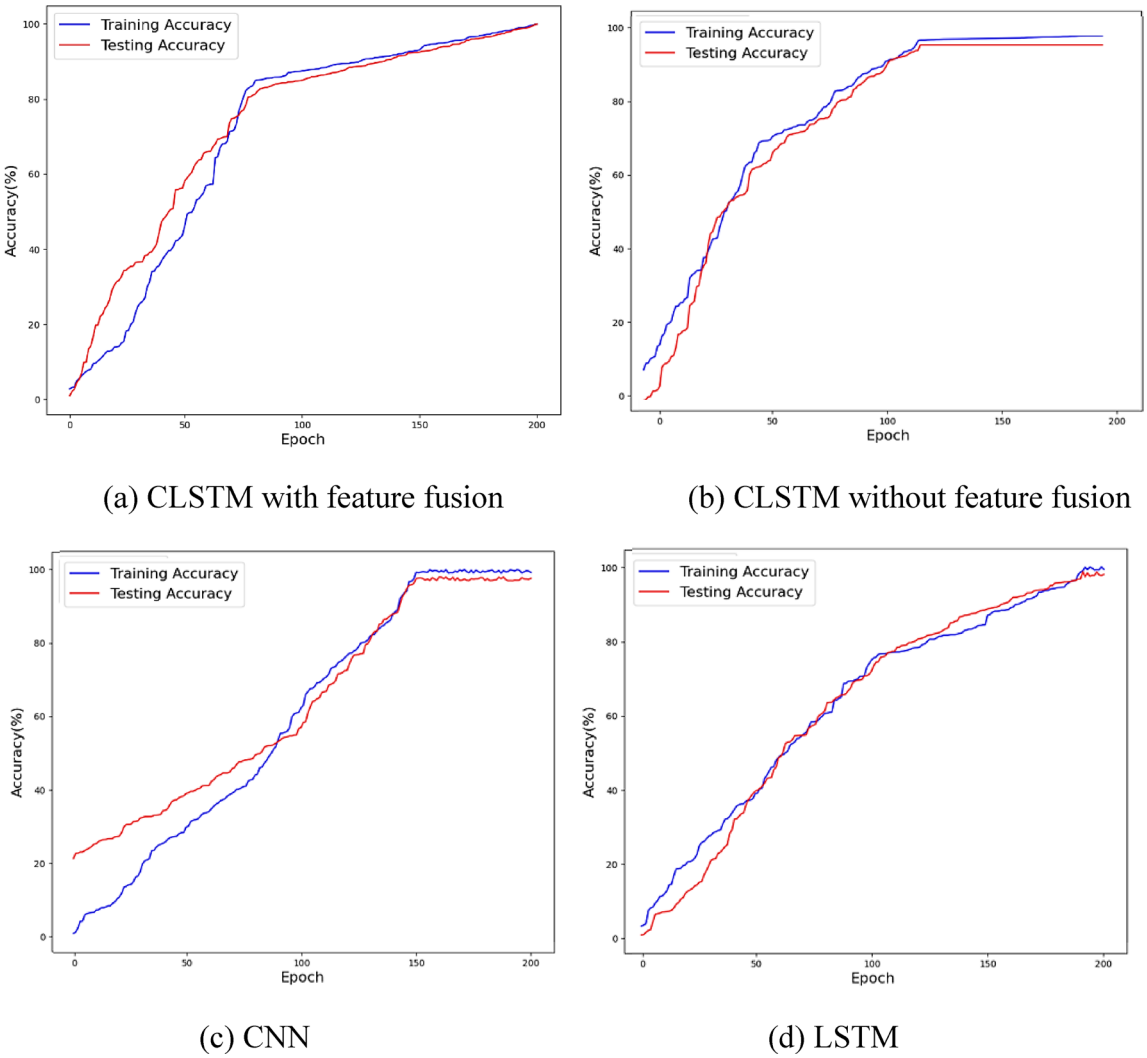

Fig. 5. Accuracy for AD detection: (**a**) CLSTM with feature fusion; (**b**) CLSTM without feature fusion; (**c**) CNN; (**d**) LSTM.

The loss is a popular statistic for model fit to training data. Model performance improves with lower loss levels. Figure 6a shows a 0.02 loss value for the CLSTM model with feature fusion. The CLSTM model, which uses feature fusion and convolutional and LSTM layers, predicts Alzheimer's disease effectively. The low loss number indicates that the model captures relevant input data patterns and correlations, resulting in more accurate predictions. However, Fig. 6b shows a CLSTM model without feature fusion with a loss value of 0.5. The CLSTM model's lack of feature fusion may reduce its capacity to gather essential information and lead to less accurate Alzheimer's disease detection predictions. The model struggles to match training data due to the larger loss.

Figure 6c shows a CNN model with 0.48 loss. The CNN approach, which employs convolutional layers to detect spatial patterns, has a modest loss. CNN works well in Alzheimer's disease detection, but not as well as CLSTM with feature fusion. The final LSTM model in Fig. 6d has a loss value of 2.8. The temporal dependencies-focused LSTM model has a greater loss value than the others. This shows that the LSTM model may not capture the key patterns and correlations in Alzheimer's disease data, resulting in less accurate predictions.

The effectiveness of the classification models is visually represented in Fig. 7 through the confusion matrix for Alzheimer's disease detection. These values are vital for assessing the accuracy and effectiveness of the models in distinguishing between AD and non-AD cases. Moving on to Fig. 7, it displays the results of various models for Alzheimer's disease detection. In Fig. 7a, a CLSTM model with feature fusion achieves an accuracy of 96% for AD cases and 100% for non-AD cases. The incorporation of feature fusion, which combines spectral-based features with those extracted by a CNN, improves the CLSTM model's performance in accurately identifying both AD and non-AD instances.

In Fig. 7b, a CLSTM model without feature fusion is displayed, achieving an accuracy of 98% for AD cases and 97% for non-AD cases. Although slightly lower than the model with feature fusion, it still demonstrates strong performance in distinguishing between AD and non-AD cases. Figure 7c showcases a CNN model, which achieves an accuracy of 96% for AD cases and 94% for non-AD cases. The CNN model shows its capability in

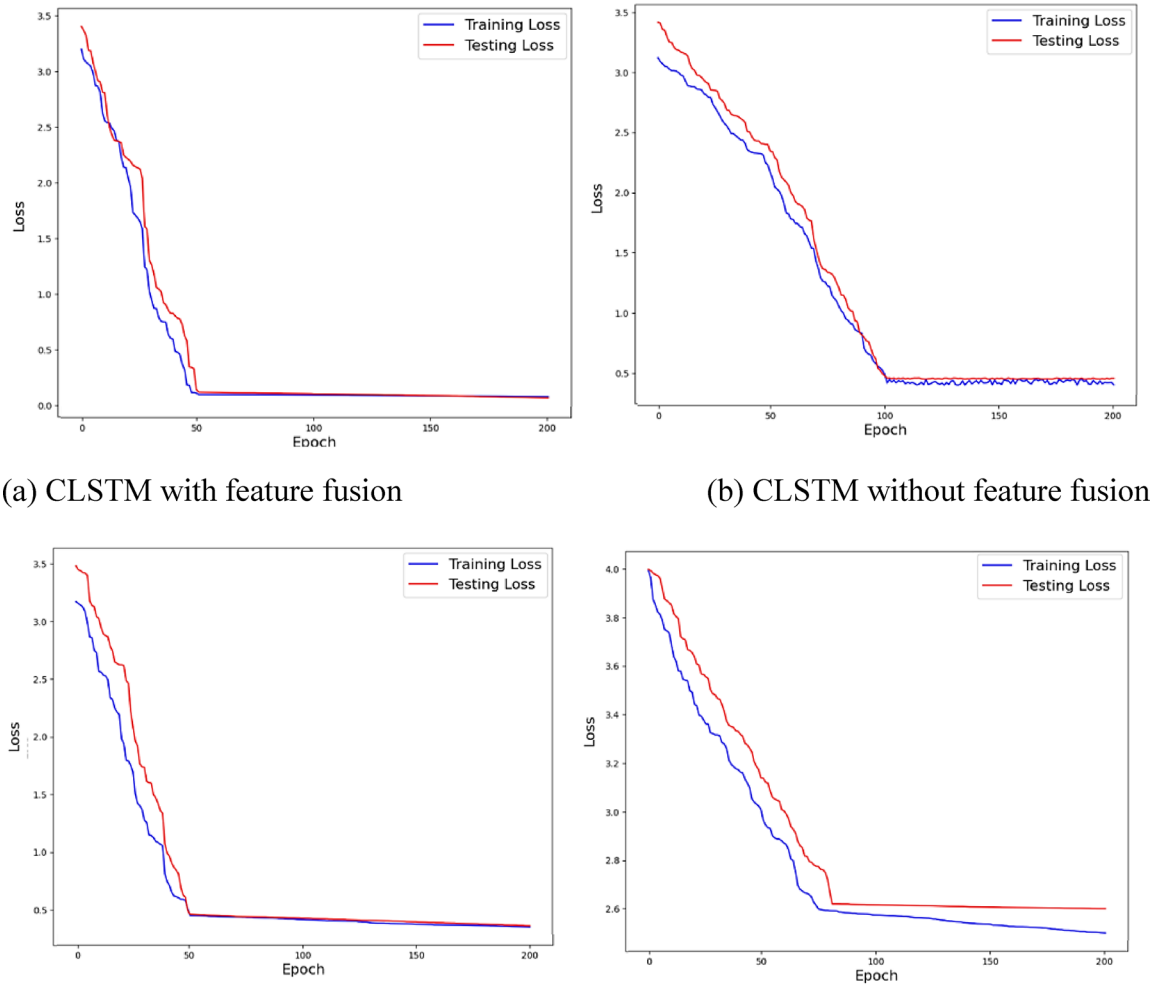

Fig. 6. Loss on for AD detection: (**a**) CLSTM with feature fusion; (**b**) CLSTM without feature fusion; (**c**) CNN; (**d**) LSTM.

accurately classifying instances of AD and non-AD based on the extracted features. Finally, Fig. 7d presents an LSTM model, achieving an accuracy of 93% for AD cases and 92% for non-AD cases. The LSTM model exemplifies its ability to capture temporal dependencies and perform well in classifying AD and non-AD instances. These results highlight the effectiveness of the CLSTM model with feature fusion, closely followed by the CLSTM model without feature fusion, in accurately detecting Alzheimer's disease. The CNN and LSTM models also display good performance, but with slightly lower accuracies.

Table 7 presents the state-of-the-art comparison of deep learning models that process EEG data. Model[43] employs SVM to classify EEG based on labels, achieving an accuracy of 92%. The deep learning models[44,45] utilise feature extraction and fusion techniques. The accuracy of these models ranges from 97.9% to 98%, but a research gap for the best feature fusion model still exists. To foster innovation in classification, novel power density spectral features are fused with deep learning features. This proposed model is lightweight, and the simple processing steps make it more intriguing. With its less complex nature, the proposed model achieves an accuracy of 99.8%.

Conclusion

This study proposes a novel feature fusion framework for the efficient detection of Alzheimer's disease (AD) from EEG, combining spectral features and deep features. EEG data were examined for spectrum and complexity to generate an AD diagnosis. Deep learning was used to analyse features from complicated datasets using convolution and pooling operations. Spectral-based feature, a modified convolutional network, and the Convolutional Long Short-Term Network (FF-CLSTM) were used for feature fusion. This investigation yielded encouraging results. FF-CLSTM diagnosed AD with 99.8% accuracy, precision of 99% and 100% classification results on normal and affected images. The new networks outperformed earlier research in classification accuracy and class size across

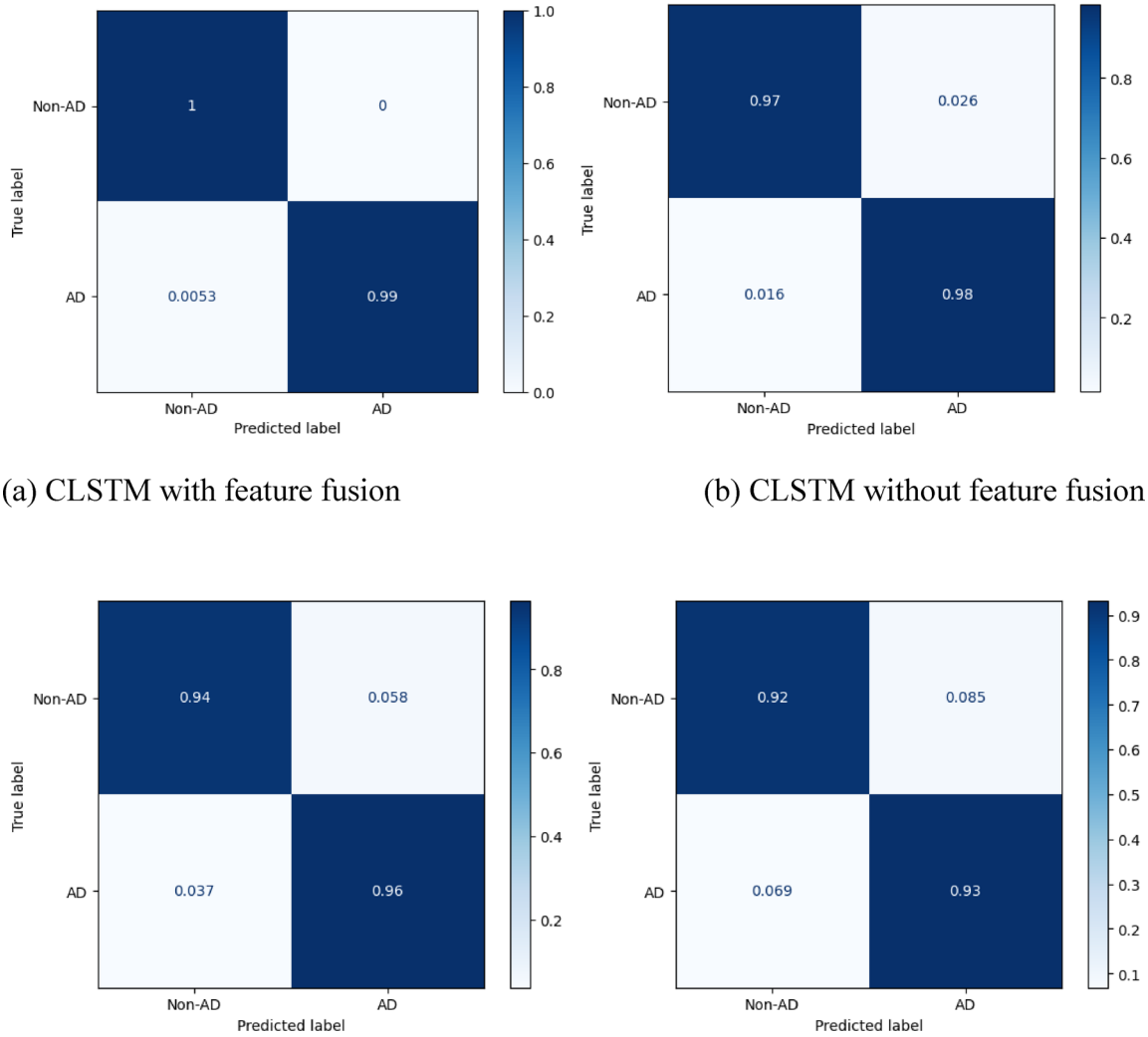

Fig. 7. Confusion matrix for Alzheimer's disease detection. (**a**) CLSTM with feature fusion, (**b**) CLSTM without feature fusion, (**c**) CNN, (**d**) LSTM.

References	Model	Feature fusion	Accuracy (%)
Yu et al., 2024[43]	SVM	no	92
Nour et al., 2024[44]	Deep ensemble learning + 2DCNN	No	97.9
Jain et al., 2025[45]	Synchrosqueezing transform and deep transfer learning	Image + Time domain	98.5
Ohal et al., 2025[46]	Statistical + SVM Time domain + SVM Frequency domain + SVM	Yes	92 87 87
Proposed	Convolutional LSTM	Power density feature + CNN features	99.8

Table 7. Comparison of state-of-the-art models.

comparable datasets. The suggested EEG-based AD diagnostic approach has great promise. Deep learning-based networks outperformed classic machine learning methods, demonstrating the value of advanced algorithms and models in Alzheimer's disease (AD) diagnosis. Deep learning and feature fusion have shown the potential of EEG for early Alzheimer's disease (AD) screening and analysis. This finding supports the growing body of AD diagnostic research and emphasizes the importance of modern computational methods for accuracy and efficiency. The findings encourage further study and the development of new diagnostic procedures to help detect and treat Alzheimer's disease early, enhancing quality of life for patients and their families.

The current study has demonstrated promising results using a deep learning-based approach with feature fusion. Future work can expand the dataset by including a larger number of subjects with diverse demographics and characteristics. This will provide a more comprehensive understanding of EEG designs associated with Alzheimer's disease (AD) and improve the generalizability of the developed models. Since Alzheimer's is a degenerative illness, keeping a close eye on a patient from the start is essential for effective intervention. Future research can involve longitudinal studies that track individuals over time to capture the temporal progression of EEG biomarkers. This will enable the development of models that can predict disease progression and assess the efficacy of treatments.

Data availability

The datasets generated during and/or analysed during the current study are available in the repository[https://github.com/OpenNeuroDatasets/ds004504].

Received: 21 June 2025; Accepted: 2 January 2026
Published online: 01 February 2026

References

1. OpenNeuro dataset: https://github.com/OpenNeuroDatasets/ds004504
2. Jeong, J. EEG dynamics in patients with Alzheimer's disease. *Clin. Neurophysiol.* **115**, 1490–1505 (2004).
3. Petersen, R. C. Early diagnosis of Alzheimer's disease: Is MCI too late. *Curr. Alzheimer Res.* **6**, 324–330 (2009).
4. Petersen, R. C. Mild cognitive impairment as a diagnostic entity. *J. Intern. Med.* **256**, 183–194 (2004).
5. Gauthier, S. et al. Mild cognitive impairment. *Lancet* **367**, 1262–1270 (2006).
6. Biagetti, G. et al. Classification of Alzheimer's disease from structural magnetic resonance imaging using particle-Bernstein polynomials algorithm. *Smart Innov. Syst. Technol.* **143**, 49–62 (2019).
7. Tsolaki, A., Kazis, D., Kompatsiaris, I., Kosmidou, V. & Tsolaki, M. Electroencephalogram and Alzheimer's disease: Clinical and research approaches. *Int. J. Alzheimer's Dis.* **2014**, 349249 (2014).
8. Kulkarni, N. N. & Bairagi, V. K. Electroencephalogram-based diagnosis of Alzheimer's Disease. In *Proceedings of the 2015 IEEE 9th International Conference on Intelligent Systems and Control (ISCO), Coimbatore, India* 1–5 (2015).
9. Falk, T. H., Fraga, F. J., Trambaiolli, L. & Anghinah, R. EEG amplitude modulation analysis for semi-automated diagnosis of Alzheimer's disease. *EURASIP J. Adv. Signal Process.* **2012**, 192 (2012).
10. Dauwels, J., Vialatte, F. & Cichocki, A. Diagnosis of Alzheimer's disease from EEG signals: Where are we standing?. *Curr. Alzheimer Res.* **7**, 487–505 (2010).
11. Fiscon, G., Weitschek, E., Felici, G., Bertolazzi, P., De Salvo, S., Bramanti, P. & De Cola, M. C. Alzheimer's disease patients classification through EEG signals processing. In *Proceedings of the 2014 IEEE Symposium on Computational Intelligence and Data Mining (CIDM), Orlando, FL, USA* 105–112 (2014).
12. Lehmann, C. et al. Application and comparison of classification algorithms for recognition of Alzheimer's disease in electrical brain activity (EEG). *J. Neurosci. Methods* **161**, 342–350 (2007).
13. Houmani, N. et al. Diagnosis of Alzheimer's disease with Electroencephalography in a differential framework. *PLoS ONE* **13**, e0193607 (2018).
14. Beckett, L. A., Harvey, D. J., Gamst, A., Donohue, M., Kornak, J., Zhang, H. & Kuo, J. H. Alzheimer's disease neuroimaging initiative. In *The Alzheimer's Disease Neuroimaging Initiative: Annual change in biomarkers and clinical outcomes* vol 6, pp 257–264 (Alzheimers Dement, 2010).
15. Goenka, S. T. Deep learning for Alzheimer prediction using brain biomarkers. *Artif. Intell. Rev.* **54**, 4827–4871 (2021).
16. Sid, H. H. & Bryant, E. O. Blood-based biomarkers for Alzheimer disease: Mapping the road to the clinic. *Nat. Rev. Neurol.* **14**, 639–652 (2018).
17. Afzal, S. et al. Alzheimer disease detection techniques and methods: A review. *Int. J. Interact. Multimed. Artif. Intell.* **6**, 26–38 (2021).
18. Marwa, E. G., Moustafa, H. E. D., Khalifa, F., Khater, H. & AbdElhalim, E. An MRI-based deep learning approach for accurate detection of Alzheimer's disease. *Alex. Eng. J.* **63**, 211–221 (2023).
19. Bandyopadhyay, A., Ghosh, S., Bose, M., Singh, A., Othmani, A. & Santosh, K. C. Alzheimer's disease detection using ensemble learning and artificial neural networks. In *Proceedings of the Recent Trends in Image Processing and Pattern Recognition, 5th International Conference, RTIP2R 2022, Kingsville, TX, USA* 12–21 (2022).
20. Balaji, P., Chaurasia, M. A., Bilfaqih, S. M., Muniasamy, A. & Alsid, L. E. G. Hybridized deep learning approach for Detecting Alzheimer's disease. *Biomedicines* **11**, 149 (2023).
21. Goel, T., Sharma, R., Tanveer, M., Suganthan, P. N., Maji, K. & Pilli, R. Multimodal Neuroimaging based Alzheimer's disease diagnosis using evolutionary RVFL classifier. *IEEE J. Biomed. Health Inform.* (2023).
22. Rahim, N. et al. Prediction of Alzheimer's progression based on multimodal Deep-Learning-based fusion and visual Explainability of time-series data. *Inf. Fusion* **92**, 363–388 (2023).
23. Fouladi, S., Safaei, A. A., Arshad, N. I., Ebadi, M. J. & Ahmadian, A. The use of artificial neural networks to diagnose Alzheimer's disease from brain images. *Multimed. Tools Appl.* **81**, 37681–37721 (2022).
24. Fouladi, S., Safaei, A. A., Mammone, N., Ghaderi, F. & Ebadi, M. J. Efficient deep neural networks for classification of Alzheimer's disease and mild cognitive impairment from scalp EEG recordings. *Cogn. Comput.* **14**, 1247–1268 (2022).
25. Ieracitano, C., Mammone, N., Hussain, A. & Morabito, F. C. A novel multi-modal machine learning based approach for automatic classification of EEG recordings in dementia. *Neural Netw.* **123**, 176–190 (2020).
26. Cassani, R., Estarellas, M., San-Martin, R., Fraga, F. J. & Falk, T. H. Systematic review on resting-state EEG for Alzheimer's disease diagnosis and progression assessment Dis. *Markers* **2018**, 1–26 (2018).
27. Ieracitano, C., Mammone, N., Bramanti, A., Hussain, A. & Morabito, F. C. A convolutional neural network approach for classification of dementia stages based on 2D-spectral representation of EEG recordings. *Neurocomputing* **323**, 96–107 (2019).
28. Caligiore, D., Silvetti, M., DâAZAmelio, M., Puglisi-Allegra, S. & Baldassarre, G. Computational modeling of catecholamines dysfunction in Alzheimer's disease at pre-plaque stage. *J. Alzheimers Dis.* **77**, 275–290 (2020).
29. Jones, D. et al. A computational model of neurodegeneration in Alzheimer's disease. *Nat. Commun.* **13**, 1643. https://doi.org/10.1038/s41467-022-29047-4 (2022).
30. Yang, S. et al. SAM: a unified self-adaptive multicompartmental spiking neuron model for learning with working memory. *Front. Neurosci.* **16**, 850945. https://doi.org/10.3389/fnins.2022.850945 (2022).
31. Yang, S., Tan, J. & Chen, B. Robust spike-based continual meta-learning improved by restricted minimum error entropy criterion. *Entropy* **24**, 455. https://doi.org/10.3390/e24040455 (2022).
32. Vu, T. H., Ikechukwu, O. M. & Ben Abdallah, A. Faulttolerant spike routing algorithm and architecture for three dimensional NoC-based neuromorphic systems. *IEEE Access* **7**, 90436–90452. https://doi.org/10.1109/ACCESS.2019.2925085 (2019).

33. Yang, S., Wang, J., Deng, B., Azghadi, M. R. & Linares-Barranco, B. Neuromorphic context-dependent learning framework with fault-tolerant spike routing. *IEEE Trans. Neural Netw. Learn. Syst.* https://doi.org/10.1109/TNNLS.2021.3084250 (2021).
34. Hjorth, B. EEG analysis based on time domain properties. *Electroencephalogr. Clin. Neurophysiol.* **29**(3), 306–310 (1970).
35. Chen, J. et al. EEG-based multi-band functional connectivity using corrected amplitude envelope correlation for identifying unfavorable driving states. *Comput. Methods Biomech. Biomed. Eng.* 1–13 (2025).
36. Tang, L., Liu, L., Li, G., Jiang, P., Wang, Y., & Li, J, Expression profiles of long noncoding RNAs in intranasal LPS-mediated Alzheimer's disease model in mice. *BioMed. Res. Int.* (2019).
37. Shi, S. & Liu, W. B2-ViT Net: Broad vision transformer network with broad attention for seizure prediction. *IEEE Trans. Neural Syst. Rehabil. Eng.* **32**, 178–188 (2024).
38. Han, L., Wei, S., Wang, R., Liu, Y., Zhong, Y., Fu, J., Luo, H., & Bao, M. Apelin-13-mediated upregulation of METTL3 ameliorates Alzheimer's disease via inhibiting neuroinflammation through m6A-dependent regulation of lncRNA BDNF-AS. *Biomolecules* **15**(8), (2025).
39. Zhang, S. et al. The intricate microbial-gut-brain axis in Alzheimer's disease: A review of microbiota-targeted strategies. *Food Funct.* **16**(21), 8320–8344 (2025).
40. Peraza, L. R., Weatheritt, J. & Wolz, R. A machine learning-based quality control tool for functional MRI images. *Alzheimers Dement.* **19**, e062768 (2023).
41. More, S. et al. Brain-age prediction: A systematic comparison of machine learning workflows. *Neuroimage* **270**, 119947 (2023).
42. Safi, M. S. & Safi, S. M. M. Early detection of Alzheimer's disease from EEG signals using Hjorth parameters. *Biomed. Signal Process. Control.* **65**, 102338 (2021).
43. Yu, W. Y. et al. Comparative analysis of machine learning algorithms for Alzheimer's disease classification using EEG signals and genetic information. *Comput. Biol. Med.* **176**, 108621 (2024).
44. Nour, M., Senturk, U. & Polat, K. A novel hybrid model in the diagnosis and classification of Alzheimer's disease using EEG signals: Deep ensemble learning (DEL) approach. *Biomed. Signal Process. Control* **89**, 105751 (2024).
45. Jain, S. & Srivastava, R. Enhanced EEG-based Alzheimer's disease detection using synchrosqueezing transform and deep transfer learning. *Neuroscience* (2025).
46. Ohal, H. S. & Mantri, S. Exploring EEG-based biomarkers for improved early Alzheimer's disease detection: A feature-based approach utilizing machine learning. *Meas.: Sens.* 101403 (2024).
47. Chen, J., Fan, F., Wei, C., Polat, K. & Alenezi, F. Decoding driving states based on normalized mutual information features and hyperparameter self-optimized Gaussian kernel-based radial basis function extreme learning machine. *Chaos, Solitons Fractals* **199**, 116751 (2025).
48. Chen, J., Cui, Y., Wei, C., Polat, K. & Alenezi, F. Driver fatigue detection using EEG-based graph attention convolutional neural networks: An end-to-end learning approach with mutual information-driven connectivity. *Appl. Soft Comput.* 114097 (2025).
49. Chen, J., Cui, Y., Wei, C., Polat, K. & Alenezi, F. Advances in EEG-based emotion recognition: Challenges, methodologies, and future directions. *Appl. Soft Comput*. 113478 (2025).

Acknowledgements

This research was supported by a grant of the project for 'Research and Development for Enhancing Infectious Disease Response Capacity in Medical & Healthcare settings', funded by the Korea Disease Control and Prevention Agency, the Ministry of Health & Welfare, Republic of Korea (grant number : RS-2025-02310471).

Author contributions

B.Hemalatha: ** Conceptualization, Methodology, Formal analysis, Validation, Resources, Supervision, Writing - original draft, Writing - review & editing.Venkatachalam K: ** Validation, Resources, Supervision, Writing - original draft, Writing - review & editing.**Siuly Siuly: ** Formal analysis, Validation, Resources, Supervision, Writing - original draft, Writing - review & editing.**Jaehyuk Cho: ** Validation, Resources, Writing - original draft, Writing - review & editing.

Funding

No funding was received for this study.

Declarations

Competing interests

The authors declare no competing interests.

Ethics approval and consent to participate

Not applicable.

Consent for publication

Not applicable.

Human and animals rights

We confirm that our study did not involve any experiments on humans, human tissue samples, or animals. Therefore, ethical approval and informed consent were not applicable to this research.

Additional information

Correspondence and requests for materials should be addressed to B.H. or J.C.

Reprints and permissions information is available at www.nature.com/reprints.

Publisher's note Springer Nature remains neutral with regard to jurisdictional claims in published maps and institutional affiliations.

Open Access This article is licensed under a Creative Commons Attribution-NonCommercial-NoDerivatives 4.0 International License, which permits any non-commercial use, sharing, distribution and reproduction in any medium or format, as long as you give appropriate credit to the original author(s) and the source, provide a link to the Creative Commons licence, and indicate if you modified the licensed material. You do not have permission under this licence to share adapted material derived from this article or parts of it. The images or other third party material in this article are included in the article's Creative Commons licence, unless indicated otherwise in a credit line to the material. If material is not included in the article's Creative Commons licence and your intended use is not permitted by statutory regulation or exceeds the permitted use, you will need to obtain permission directly from the copyright holder. To view a copy of this licence, visit http://creativecommons.org/licenses/by-nc-nd/4.0/.

© The Author(s) 2026